Optical in situ size determination of single lanthanide-ion doped oxide nanoparticles

Didier Casanova, Domitile Giaume, Emmanuel Beaurepaire, Thierry Gacoin, Jean-Pierre Boilot, Antigoni Alexandrou

Optical *in situ* size determination of single lanthanide-ion doped oxide nanoparticles

Didier Casanova
Laboratory for Optics and Biosciences, CNRS UMR7645, INSERM U696, Ecole Polytechnique, F-91128 Palaiseau Cedex, France

Domitille Giaume
Laboratory of Condensed Matter Physics, CNRS UMR7643, Ecole Polytechnique, F-91128 Palaiseau Cedex, France

Emmanuel Beaurepaire
Laboratory for Optics and Biosciences, CNRS UMR7645, INSERM U696, Ecole Polytechnique, F-91128 Palaiseau Cedex, France

Thierry Gacoin and Jean-Pierre Boilot
Laboratory of Condensed Matter Physics, CNRS UMR7643, Ecole Polytechnique, F-91128 Palaiseau Cedex, France

Antigoni Alexandrou[a)]
Laboratory for Optics and Biosciences, CNRS UMR7645, INSERM U696, Ecole Polytechnique, F-91128 Palaiseau Cedex, France

(Received 27 July 2006; accepted 9 November 2006; published online 18 December 2006)

We show that the size of a lanthanide-ion doped nanoparticle can be accurately determined from its luminosity. The optically determined size distribution is in very good agreement with the distribution obtained from transmission electron microscopy. These data confirm that single nanoparticles are visualized in microscopy experiments. Nanoparticles as small as 13 nm are detectable with integration times of 500 ms. © *2006 American Institute of Physics*.
[DOI: 10.1063/1.2405871]

Fluorescence microscopy based on biomolecule labeling with a fluorophore is one of the basic tools for understanding cellular processes. Ideally, such a fluorescent biological label should be water soluble, photostable, and small in order to minimize perturbation of the biomolecule function. In practice, a compromise is made between size, brightness, and photostability. For example, organic fluorophores are small but photobleach very rapidly (within a few seconds in typical single-molecule experiments). Photostable nanocrystals, such as colloidal quantum dots[1–3] (QDs) and lanthanide-doped oxide nanoparticles[4,5] (NPs) have been proposed as alternative systems.[6–10] These nanocrystal labels are larger (10–30 nm) but much more photostable (observation during several tens of minutes).

The size of these nanocrystal labels is usually determined using transmission electron microscopy (TEM) which necessitates expensive equipment or dynamic light scattering experiments which are difficult to interpret in the case of polydisperse solutions. Furthermore, no size determination of individual fluorescent nanoparticles in single-molecule experiments is available at the moment. Such an *in situ* size determination is important for assessing the presence of single nanoparticles (aggregation state) and the perturbation of the biomolecule behavior induced by the nanoparticle label.

We here present a simple *in situ* size determination at the single nanoparticle level for lanthanide-doped oxide nanoparticles based on the fact that the nanoparticle luminosity is proportional to the number of dopants, i.e., to the volume of the nanoparticle. The good agreement between the optically determined size distribution and the one measured using TEM confirms the validity of this approach. We furthermore determine the smallest detectable NP size by using simulated optical images.

We have recently demonstrated that lanthanide-doped oxide NPs, $Y_{1-x}Eu_xVO_4$, are detectable at the single-particle level and show no emission intermittency.[6] This system has additional attractive characteristics: synthesis directly in water,[5] long excited-state lifetime rendering retarded detection schemes[6] and lifetime measurements particularly straightforward,[11] and narrow emission linewidth.[12] In contrast to QDs, the emission wavelength is independent of size because the electronic states involved are highly localized at the Eu^{3+} ion.[13] The latter property is also responsible for the extremely narrow emission (<10 nm).

$Y_{0.6}Eu_{0.4}VO_4$ NPs with an average diameter of approximately 35 nm were synthesized according to the protocol described in Ref. 5. Two centrifugations at 11400 g for 10 min each and retention of the supernatant allowed selecting a subset of smaller NPs. A drop of NP solution was deposited on a carbon-coated copper grid and then heated at 120 °C to evaporate the solvent. The NP size distribution was determined by TEM (Philips CM 30 microscope operated at 300 keV, 0.235 nm resolution). For optical microscopy imaging, the NPs were spin coated on a silica coverslip at sufficiently low concentration to enable observation of individual NPs using an inverted wide-field microscope (Zeiss Axiovert 100), a numerical aperture=1.3, 100×, oil-immersion objective, a subsequent image magnification of

[a)]Electronic mail: antigoni.alexandrou@polytechnique.fr; URL: http://www.lob.polytechnique.fr

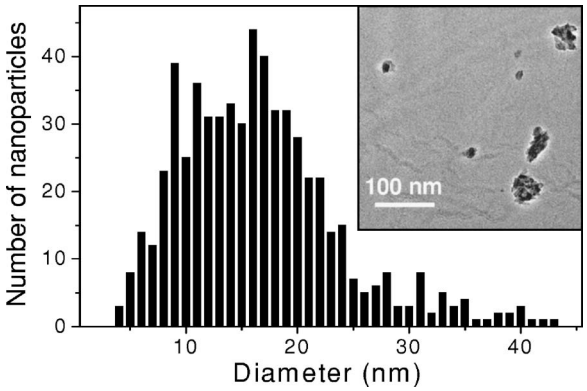

FIG. 1. Size distribution of $Y_{0.6}Eu_{0.4}VO_4$ nanoparticles determined from TEM images (see inset). Total number of NPs: 603.

8/5 using two lenses, and a liquid-nitrogen cooled back-illuminated charge-coupled device (CCD) camera (Princeton Instruments LN/CCD-400-PB, 20 μm/pixel). We used the 465.8 nm Ar^+-ion laser line coinciding with the Eu^{3+} $^7F_{0,1}$-$^5D_2$ transition to excite the $Y_{0.6}Eu_{0.4}VO_4$ NPs.[6] Their emission at 617 nm (Eu^{3+} $^5D_0$-$^7F_2$ transition) was detected.

The inset of Fig. 1 represents a typical TEM image showing seven NPs. The NPs being nonspherical, we define the NP diameter (size) as the diameter of a sphere of equal volume. A short and a long axis can be measured for each NP surface seen in the TEM images. The third axis of the ellipsoid was taken equal to the diameter of a circle of equal surface. Nanoparticles tend to aggregate when deposited on the hydrophobic carbon grid. Only nanoparticles clearly identified as individual objects were considered for determining the size distribution. We obtained a NP size distribution with a maximum at 16 nm (Fig. 1).[14]

Optical microscopy images were recorded at different locations on a nanoparticle-coated coverslip (integration time: 500 ms; see inset of Fig. 2). An image analysis program was used to identify diffraction-limited bright spots with a total number of pixels between 5 and 84 and to determine their position and the corresponding total photon number. The nanoparticle density and the upper spot-size value are chosen so as to correctly detect the total photon number (taking into account $\sim[3\times$full width at half maximum (FWHM)$]^2$ pixels) while avoiding detection of two nearby nanoparticles as a single one. The analysis procedure involves sequential high-pass/

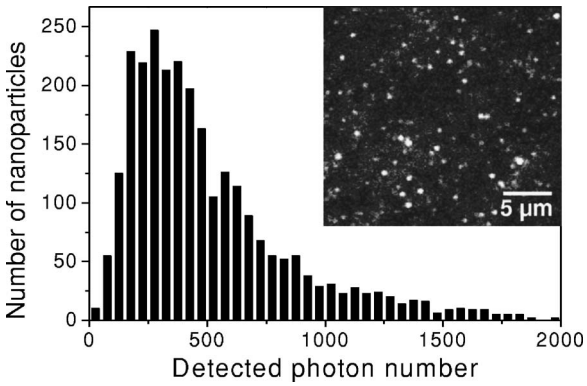

FIG. 2. Luminosity distribution of $Y_{0.6}Eu_{0.4}VO_4$ nanoparticles determined from optical microscopy images with integration time of 500 ms (see inset). Total number of NPs: 3255.

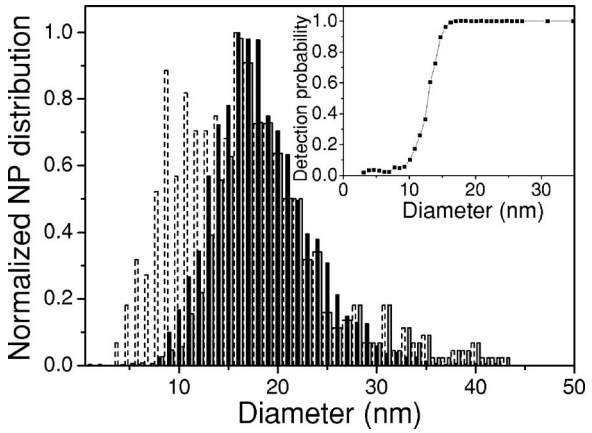

FIG. 3. Normalized size distribution calculated from experimental optical microscopy images (black) in comparison to that determined from electron microscopy images (dashed) multiplied by the calculated optical detection probability shown in the inset (gray).

low-pass spatial filtering and generation of a threshold-based binary mask.[15,16] Particular care was taken to correctly determine the threshold (by taking into account the excitation intensity variations across the image) and the total NP photon number. We thus obtained the NP luminosity distribution shown in Fig. 2.

In the case of direct Eu^{3+} excitation, the number of emitted photons per second is proportional to the number of Eu^{3+} ions per NP which in turn is proportional to the NP volume, the Eu^{3+} concentration, and the luminescence quantum yield q. Note that the quantum yield decreases for Eu^{3+} concentrations above 30%.[12] The number of detected photons per second N_{det} is thus given by

$$N_{\mathrm{det}} = q\eta\frac{\sigma I}{h\nu}4x\frac{(4/3)\pi(D/2)^3}{V}, \tag{1}$$

where η is the detection efficiency of the optical setup, σ the absorption cross section of the 466 nm Eu^{3+} absorption line, I the excitation intensity, $h\nu$ the excitation photon energy, x the fraction of Y^{3+} ions replaced by Eu^{3+} ions, D the NP diameter, and V the unit cell volume of the $Y_{0.6}Eu_{0.4}VO_4$ crystal. The first fraction in Eq. (1) corresponds to the number of absorbed photons per Eu^{3+} ion, while the second is equal to the number of unit cells in a NP of diameter D. Each unit cell contains 4 VO_4^{3-} ions and $4x$ Eu^{3+} ions. In our case, $q=0.068$, $\eta=0.097$, $\sigma=1.41\times10^{-21}$ cm^2,[6] $h\nu=2.66$ eV, $x=0.4$, $V=0.323$ nm^3.[5] We used 80 mW of incident laser power at the sample plane. The intensity profile was measured using the fluorescence of an uncoated coverslip (focusing down to 33 μm). The excitation intensity for each NP based on its position with respect to the laser intensity profile could thus be determined (ranging from 2.8 to 4.4 kW/cm^2). The detected photon flux decreases upon sustained excitation.[6] The characteristic decay time was measured and used to correct the detected photon number for this effect (correction factor: 1.43 for our experimental conditions). The value used in Eq. (1) corresponds to the detected photon number in the absence of photon flux decrease.

Using Eq. (1), we converted the luminosity distribution into the optically determined size distribution shown in Fig. 3. The maximum (16 nm) and the high-size tail of this distribution are in very good agreement with those determined by TEM. Nevertheless, the presence of small NPs

(<13 nm) is underestimated in the optically determined size distribution. This is not surprising since the low photon number emitted by small nanoparticles is difficult to detect on top of the background fluorescence.

To quantify the performances of our optical setup and optimize the image analysis in terms of single NP detection, we applied our image analysis procedure to simulated images generated as follows: we considered NPs with a fixed size randomly distributed on a grid of 200×200 pixels as in the experiment. Their luminosity was calculated using Eq. (1). The signal from individual NPs was simulated by two-dimensional Gaussian profiles with a FWHM of 2.8 pixels (336 nm) as in experiments. We then added the coverslip fluorescence (FWHM: 278 pixels, i.e., 33 μm). Finally, shot noise (varying as $\sqrt{N}$, where N is the total number of detected photons) was added for each pixel. The image analysis program was then used on the simulated images. We considered that a nanoparticle was correctly detected when its x and y positions were determined with an error of less than 2 pixels. This was repeated for NP diameters ranging from 1 to 60 nm. The fraction of correctly detected NPs as a function of NP diameter is shown in the inset of Fig. 3. When we multiply the TEM-determined histogram of Fig. 1 with this size-dependent probability of detection, we obtain the gray size distribution in Fig. 3 which is in very good agreement with the optically determined distribution confirming the validity of our optical single-particle size determination (Gaussian fits of the two distributions give the same peak and width value to within 1% and 9%, respectively). Since electron microscopy data resolve single NPs, this good agreement confirms that optical microscopy experiments also detect single NPs. Since single NPs are strictly speaking not single emitters (several thousands of Eu^{3+} ions are involved), they are not single photon sources and photon antibunching measurements cannot be used to affirm the existence of single NPs. Therefore, this comparison with TEM characterization is the only way of confirming that we indeed detect single objects.

We define the size detection limit of our setup as the NP diameter for which the probability of correct detection is 0.5. We thus find that the size limit is 13 nm for our experimental conditions. With an integration time of 100 ms instead of 500 ms, it would be 22 nm. With a quantum yield of 14%,[5] an integration time of 500 ms and an excitation intensity of 12 kW/cm^2, it would be 7 nm. The total photon number is slightly underestimated because of the threshold in the image analysis procedure. For nanoparticles larger than 16 nm, this error is less than 10%. Taking into account the errors of the other parameters in Eq. (1), we find an error of 9% (15%) in the diameter (volume) determination. The localization precision is 28(56) nm for 20(16) nm NPs.

The number of photons detected per second is an important issue for single-molecule observations. It is related to the absorption coefficient, the quantum yield, and the excited-state lifetime. Indeed, the shorter the lifetime, the faster the emitter returns to the ground state and is available for further excitation. This, however, is true only close to saturation. In our case, because of the large number of Eu^{3+} ions present in each nanoparticle, typical intensities used are more than two orders of magnitude below the saturation intensity of 10^3 kW/cm^2 and the long excited-state lifetime is not a limitation for NP luminosity. The only limitations are then set by the absorption coefficient, the quantum yield, and the possibility of cell photodamage at high intensities.

We have shown that the size of single lanthanide-doped oxide NPs can be accurately determined (10% error for NPs larger than 16 nm) from the detected photon number in optical microscopy experiments in the same conditions as for single-molecule labeling experiments without complex TEM characterization. Sizes as small as 13 nm are detectable with integration times of 500 ms. We point out that the functionalization of such nanoparticles only slightly increases their size (1–2 nm) (Ref. 6) in contrast to QDs which are synthesized in organic solvents and where, in most cases, the water solubilization and functionalization layer lead to a substantial increase in size.[3] Finally, we note that the minimum detectable size could be decreased by exciting the oxide matrix in the UV (where the absorption coefficient is much higher)[6] and by performing time-gated detection in order to increase the signal-to-background ratio.

The authors thank the Fonds National pour la Science (AC Nanosciences and AC Dynamique et Réactivité des Assemblages Biologiques) and the DGA (Délégation Générale pour l'Armement) for financial support.

[1] M. Bruchez, M. Moronne, P. Gin, S. Weiss, and A. P. Alivisatos, Science **281**, 2013 (1998).
[2] W. C. W. Chan and S. Nie, Science **281**, 2016 (1998).
[3] X. Michalet, F. F. Pinaud, L. A. Bentolila, J. M. Tsay, S. Doose, J. J. Li, G. Sundaresan, A. M. Wu, S. S. Gambhir, and S. Weiss, Science **307**, 538 (2005).
[4] M. Haase and K. Riwotzki, J. Phys. Chem. B **102**, 10129 (1998).
[5] A. Huignard, T. Gacoin, and J.-P. Boilot, Chem. Mater. **12**, 1090 (2000).
[6] E. Beaurepaire, V. Buissette, M.-P. Sauviat, D. Giaume, K. Lahlil, A. Mercuri, D. Casanova, A. Huignard, J.-L. Martin, T. Gacoin, J.-P. Boilot, and A. Alexandrou, Nano Lett. **4**, 2079 (2004).
[7] G. Yi, H. Lu, S. Zhao, Y. Ge, W. Yang, D. Chen, and L.-H. Guo, Nano Lett. **4**, 2191 (2004).
[8] C. Louis, R. Bazzi, C. A. Marquette, J.-L. Bridot, S. Roux, G. Ledoux, B. Mercier, L. Blum, P. Perriat, and O. Tillement, Chem. Mater. **17**, 1673 (2005).
[9] D. Dosev, M. Nichkova, M. Liu, B. Guo, G.-Y. Liu, B. D. Hammock, and I. M. Kennedy, J. Biomed. Opt. **10**, 064006 (2005).
[10] F. Wang, W. B. Tan, Y. Zhang, X. P. Fan, and M. Q. Wang, Nanotechnology **17**, R1 (2006).
[11] D. Casanova, D. Giaume, T. Gacoin, J.-P. Boilot, and A. Alexandrou, J. Phys. Chem. B **110**, 19264 (2006).
[12] A. Huignard, V. Buissette, A.-C. Franville, T. Gacoin, and J.-P. Boilot, J. Phys. Chem. B **107**, 6754 (2003).
[13] G. Blasse and B. C. Grabmeier, *Luminescent Materials* (Springer, Berlin, 1994).
[14] If we consider the third axis equal to the short axis, the mean NP size differs by only 1.5 nm.
[15] S. Inoue, *Video microscopy* (Plenum, New York, 1986).
[16] R. N. Ghosh and W. W. Webb, Biophys. J. **66**, 1301 (1994).